2008 American Control Conference
Westin Seattle Hotel, Seattle, Washington, USA
June 11-13, 2008

Triple Tilting Rotor mini-UAV: Modeling and Embedded Control of the Attitude

J. Escareño, A. Sanchez, O. Garcia, R. Lozano

Abstract— **The goal of this paper is to present a novel configuration for a three-rotor mini Unmanned Aerial Vehicle (UAV). The proposed design incorporates advantageous structural features which enhance the maneuverability of the rotorcraft. The detailed mathematical model of the vehicle's attitude is obtained through the Newton-Euler formulation. In terms of control, we propose a control law which is robust with respect to dynamical couplings and adverse torques. The vehicle tilts simultaneously the three rotors to stabilize the yaw dynamics. The resulting control algorithm is simple for embedded purposes. A customized low-cost embedded system was developed to test an autonomous stabilized-attitude flight, obtaining satisfactory results.**

Index Terms— **Three-rotor aircraft, Coupled dynamics, Collective tilting, Homemade IMU, Embedded architecture, VTOL.**

I. Introduction

The growing interest on the design of rotary-wing UAVs for military and civilian applications, has encouraged industry and researchers to search for new designs, aiming at more efficient configurations in terms of size, flight range, autonomy and payload capacity.

A reliable autonomous attitude-stabilized flight is required for reconnaissance and surveillance missions, where the goal is to provide a visual perspective of "blind" areas (around the corner, over the hill). In these missions, the 3D position is usually controlled by the operator (e.g. cop/soldier at a safe location) through an on-board camera, whereas the attitude is computer-controlled.

There exists various types of rotorcrafts. Some have two rotors like the the classical helicopter or the tilting rotor aircraft. Four-rotor rotorcrafts are also very popular [2]. Other multi-rotorcrafts have even a large number or rotors as the one in [3] which has eight rotors. Some of these rotorcraft have variable pitch blades like the classical helicopter or tilting rotors [4] and have strong nonlinear couplings which increase the complexity of the controller design. Four-rotor configurations have smaller nonlinear coupling and are easier to control. In this paper we are interested in designing a rotorcraft using only three fixed pitch blade rotors which have the same manoeuvrability of four-rotor aircrafts. The reduction in the number of rotors from four to three allows to obtain more compact vehicles (backpackable UAVs) for rapid deployment, as well as longer flight autonomy.

Heudiasyc-UTC UMR 6599 Centre de Recherches de Royallieu B.P. 20529 60205 Compiegne France Tel.: + 33 (0)3 44 23 44 23 ; fax: +33 (0)3 44 23 44 77
corresponding author: rlozano@hds.utc.fr
[jescaren,asanchez,ogarcias]@hds.utc.fr

There exist few works concerning three-rotor vehicles in the literature. In [5], a body-rotating (lack of yaw control) three-rotor is presented. In this configuration the vehicle maintains the horizontal attitude by combining the aircraft's gyroscopic effect and a piezoelectric sensor, also described in the paper, in order to sense the tilt angle with respect to the horizontal orientation. An alternative three-rotor configuration is presented in [6]. In this design, the front rotors control the roll motion and provide the main lift component, whereas the tail rotor controls the pitch and yaw motion (rotor tilting). The control algorithm was run in an external PC based on the approach of the nested saturations.

In the present paper we propose a three-rotor configuration, called Delta[1], which incorporates certain structural advantages in order to improve the attitude stabilization. The proposed vehicle provides a reliable maneuverability despite the reduced number of rotors. In terms of control, we design a control strategy to stabilize the attitude of the Delta rotorcraft in presence of dynamic coupling and adverse propeller effects (the gyroscopic and blade's drag torques). Moreover, the resulting algorithm is simple for embedded purposes. The paper is organized as follows: Section II presents the detailed dynamical model of the three-rotor rotorcraft. The control strategy is presented in section III. The simulation results of the attitude stabilization are given in section IV. In section V, we describe the experimental prototype, the embedded system as well as real-time results of an autonomous attitude-stabilized flight of the Delta UAV. Finally some concluding remarks are given in section VI.

II. Delta UAV

The Delta mini-UAV has three rotors located at the same distance from the center of gravity $\mathcal{C}$. This structural feature (symmetry) allows to provide a symmetric lift contribution for the vehicle, improving its stability and payload capability. In addition, the heading is controlled by the collective tilting of the rotors.

A. Attitude dynamics

The body frame is formed by $\mathcal{B}$=$\{i_{\mathcal{C}}^{\mathcal{B}}, j_{\mathcal{C}}^{\mathcal{B}}, k_{\mathcal{C}}^{\mathcal{B}}\}$, and is attached to the vehicle, whose $\mathcal{C}$ is located at the origin of the frame. The equation that models the rotational motion of the vehicle is given by

$$\mathbb{I}\dot{\Omega}^{\mathcal{B}} + \Omega^{\mathcal{B}} \times \mathbb{I}\Omega^{\mathcal{B}} = \Gamma^{\mathcal{B}} \tag{1}$$

[1]We have chosen Delta to denote the symmetrical rotor placement on the vehicle

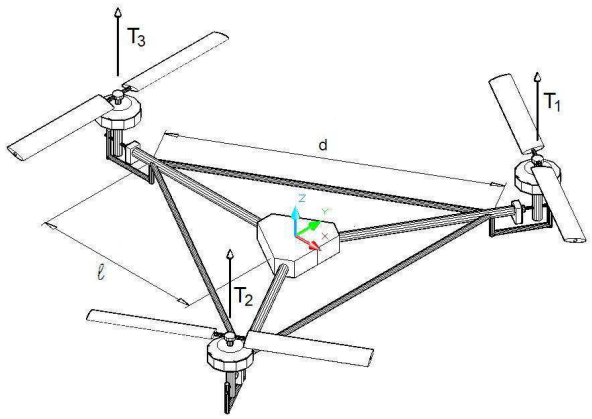

Fig. 1. Delta rotorcraft free-body scheme.

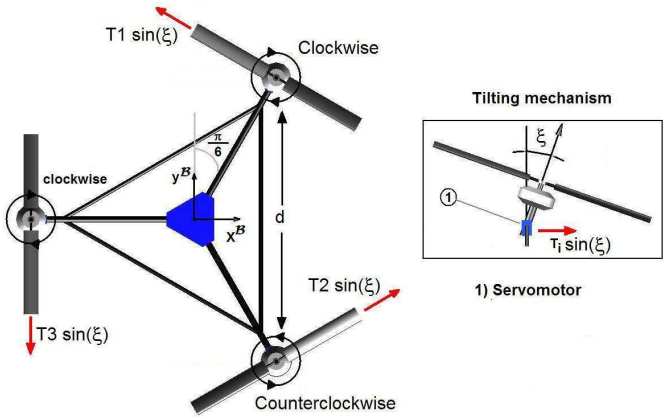

Fig. 2. Yaw motion

where the body-axis torque vector is mainly composed by a torque provided by actuators and a parasitic torque provide by propeller (gyroscopic effect, blade's drag).

$$\Gamma_c^{\mathcal{B}} = \Gamma_c^{\mathcal{B}} + \Gamma_g^{\mathcal{B}} + \Gamma_d^{\mathcal{B}} \tag{2}$$

The angular rate vector relative to body-axis ($\Omega^{\mathcal{B}} = (p, q, r)^T$) frame is related to the Euler angular rate vector ($\dot{\eta} = (\dot{\phi}, \dot{\theta}, \dot{\psi})^T$) by

$$\Omega^{\mathcal{B}} = \mathcal{W}_n \dot{\eta} \text{ with } \mathcal{W}_n = \begin{pmatrix} 1 & 0 & -s_\theta \\ 0 & c_\phi & c_\theta s_\phi \\ 0 & -s_\phi & c_\theta c_\phi \end{pmatrix} \tag{3}$$

$\mathcal{W}_n$ denotes separate rotations of the three Euler angles rate components by three different orthonormal matrices (Euler rotations)[8]-[1]. Using (3) we obtain the time derivative, given as

$$\dot{\Omega}^{\mathcal{B}} = \mathcal{W}_n \ddot{\eta} + \left(\frac{\partial \mathcal{W}_n}{\partial \phi} \dot{\phi} + \frac{\partial \mathcal{W}_n}{\partial \theta} \dot{\theta} \right) \dot{\eta}, \tag{4}$$

in (1), we obtain the detailed equation that describes the dynamical behavior of the rotational motion:

$$\mathbb{I} \left[\mathcal{W}_n \ddot{\eta} + \left(\frac{\partial \mathcal{W}_n}{\partial \phi} \dot{\phi} + \frac{\partial \mathcal{W}_n}{\partial \theta} \dot{\theta} \right) \dot{\eta} \right] + (\mathcal{W}_n \dot{\eta}) \times \mathbb{I} (\mathcal{W}_n \dot{\eta}) = \Gamma^{\mathcal{B}} \tag{5}$$

- ***Actuator torque:*** The expression that defines the actuators torque is obtained in terms of the body-axis frame.

$$\Gamma_c^{\mathcal{B}} = \ell_1^{\mathcal{B}} \times \mathbf{T}_1^{\mathcal{B}} + \ell_2^{\mathcal{B}} \times \mathbf{T}_2^{\mathcal{B}} + \ell_3^{\mathcal{B}} \times \mathbf{T}_3^{\mathcal{B}} \tag{6}$$

with

$$\begin{aligned} \ell_1^{\mathcal{B}} &= \left[\ell \sin(\tfrac{\pi}{6}), \ell \cos(\tfrac{\pi}{6}), 0 \right]^T, \\ \ell_2^{\mathcal{B}} &= \left[\ell \sin(\tfrac{\pi}{6}), -\ell \cos(\tfrac{\pi}{6}, 0 \right]^T, \\ \ell_3^{\mathcal{B}} &= \left[-\ell, 0, 0 \right]^T. \end{aligned}$$

where ℓ denotes the distance from the motor to the gravity center. To obtain the thrust vectors $\mathbf{T}_1$ and $\mathbf{T}_2$ in terms of the body axis, we consider an auxiliary frame provided by the tilting angle ξ, thus, it is required a rotation $\mathcal{R}^{\xi_y}$ about j_y. Afterwards, a fixed rotation $\mathcal{R}^{\frac{\pi}{6}}$ about k_z provided by the structure of the vehicle [see figure 2].

$$\mathcal{R}^{\xi_y} = \begin{pmatrix} \cos\xi & 0 & \sin\xi \\ 0 & 1 & 0 \\ -\sin\xi & 0 & \cos\xi \end{pmatrix} \tag{7}$$

$$\begin{aligned} \mathbf{T}_1^{\mathcal{B}} &= \mathcal{R}^{\frac{\pi}{6}} \mathcal{R}^{\xi} \mathbf{T}_1^{\xi} \\ \mathbf{T}_2^{\mathcal{B}} &= (\mathcal{R}^{\frac{\pi}{6}})^T (\mathcal{R}^{\xi})^T \mathbf{T}_2^{\xi} \end{aligned} \tag{8}$$

For $\mathbf{T}_3$ the only existing rotation is the one provided by the tilting angle ξ, but now, about $-i_x$.

$$\mathcal{R}^{\xi_x} = \begin{pmatrix} 1 & 0 & 0 \\ 0 & \cos\xi & \sin\xi \\ 0 & -\sin\xi & \cos\xi \end{pmatrix} \tag{9}$$

$$\mathbf{T}_3^{\mathcal{B}} = \mathcal{R}^{\xi_x} \mathbf{T}_3^{\xi} \tag{10}$$

From (8) and (10), the three scalar equations for the body-axis thrust can be written as

$$\begin{aligned} \mathbf{T}_1^{\mathcal{B}} &= [T_1 \cos\tfrac{\pi}{6} \sin\xi, -T_1 \sin\xi \sin\eta, T_1 \cos\xi]^T \\ \mathbf{T}_2^{\mathcal{B}} &= [-T_2 \cos\tfrac{\pi}{6} \sin\xi, -T_2 \sin\xi \sin\eta, T_2 \cos\xi]^T \\ \mathbf{T}_3^{\mathcal{B}} &= [0, T_3 \sin\xi, T_3 \cos\xi]^T \end{aligned} \tag{11}$$

Finally, using (II-A) and (11) to solve (6), we obtain the expression of the actuators vector torque:

$$\Gamma_c^{\mathcal{B}} = \begin{pmatrix} \frac{1}{2}\sqrt{3}\ell(\cos\xi)(T_1 - T_2) \\ -\frac{1}{2}\ell(\cos\xi)(T_1 + T_2 - 2T_3) \\ -\ell(\sin\xi)(T_1 + T_2 + T_3) \end{pmatrix} \tag{12}$$

- ***Gyroscopic torque:*** The rotor tilting produce an adverse torque, which can be described by the following

$$\Gamma_g^{\mathcal{B}} = -I_b \sum_{i=1}^{3} (\Omega^{\mathcal{B}} \times \omega_{b_i}^{\mathcal{B}}) \tag{13}$$

with

$$\begin{aligned} \omega_{b_1}^{\mathcal{B}} &= \mathcal{R}^{\frac{\pi}{6}} \mathcal{R}^{\xi} \omega_{b_1}^{\xi} \\ \omega_{b_2}^{\mathcal{B}} &= (\mathcal{R}^{\frac{\pi}{6}})^T (\mathcal{R}^{\xi_y})^T \omega_{b_2}^{\xi} \\ \omega_{b_3}^{\mathcal{B}} &= \mathcal{R}^{\xi_x} \omega_{b_3}^{\xi} \end{aligned}$$

where I_b and ω_{b_i} are, respectively, the inertia moment and the angular speed of the propellers.

- ***Drag torque:*** An adverse torque is also generated by the air resistance experienced by a rotating blade (drag), which can be modeled as

$$\Gamma_d^{\mathcal{B}} = \sum_{i=1}^{3} \ell_i^{\mathcal{B}} \times D_{b_i}^{\mathcal{B}} \tag{14}$$

with

$$\begin{aligned} \mathbf{D}_{b_1}^{\mathcal{B}} &= \mathcal{R}^{\frac{\pi}{6}} \mathcal{R}^{\xi_y} D_{b_1}^{\xi} \\ \mathbf{D}_{b_2}^{\mathcal{B}} &= (\mathcal{R}^{\frac{\pi}{6}})^T (\mathcal{R}^{\xi_y})^T D_{b_2}^{\xi} \\ \mathbf{D}_{b_3}^{\mathcal{B}} &= \mathcal{R}^{\xi_x} D_{b_3}^{\xi} \end{aligned}$$

III. Control strategy

In this section we present a control strategy to stabilize the attitude of the three-rotor VTOL. For this analysis we have neglected the gyroscopic and propeller-drag torques, in experimental test we will show that the proposed strategy is robust enough to deal with this terms. This control strategy splits the rotational dynamics in three subsystems: the axial, lateral and longitudinal dynamics.

- **Axial dynamics**: This dynamics correspond to the heading motion of the vehicle, which is described by the following equation:

$$I_z \ddot{\psi} = -\ell(\sin\xi)(T_1 + T_2 + T_3), \tag{15}$$

For simplicity we consider the normalized value of I_z and $\ell(T_1+T_2+T_3)$, i.e. $I_z = 1$ and $\ell(T_1+T_2+T_3) = 1$. Now, let us rewrite the vector-state representation of (15)

$$\begin{aligned} \dot{x}_{\psi_1} &= x_{\psi_2} \\ \dot{x}_{\psi_2} &= -\sin(u_\psi) \end{aligned} \tag{16}$$

where $x_{\psi_1} = \psi$,$x_{\psi_2} = \dot{\psi}$ and $u_\psi = \xi$. We propose the following control input, in order to stabilize the system (16)

$$u_\psi = \arcsin(v_\psi) \tag{17}$$

Notice that $\arcsin(v_\psi)$ is defined for values within the interval $-1 \leq v_\psi/k_\psi \leq 1$. For this reason we will bound v_ψ to this interval. To do so, we will employ a saturation-based algorithm [9], which is described next.

We define the following change of variables:

$$\begin{aligned} z_1 &= x_{\psi_2} \\ z_2 &= z_1 + x_{\psi_1} \end{aligned} \tag{18}$$

and $v_\psi = \sigma_a(z_1 + \sigma_b(z_2))$. Then, the control input (17) becomes

$$u_\psi = \arcsin(\sigma_a(z_1 + \sigma_b(z_2))) \tag{19}$$

where σ_n is a saturation function defined as

$$\sigma_\eta(s) = \begin{cases} \eta & s > \eta \\ s & -\eta \leq s \leq \eta \\ -\eta & s < -\eta \end{cases}$$

We will show that the control law (19) stabilizes the system (15) around the origin.

Stability analysis

Let us consider the following positive function $V_1 = \frac{1}{2} z_1^2$ where $z_1 = x_{\psi_2}$. Thus, $\dot{z}_1 = \dot{x}_{\psi_2} = -\sin(u_\psi)$ and thus $\dot{V}_1$ is

$$\dot{V}_1 = -z_1 \sigma_a(z_1 + \sigma_b(z_2)) \tag{20}$$

note that if $|z_1| > a$ and $a > b$ then $\dot{V}_1 < 0$. Therefore, there exists a finite time t_1 such that for $t > t_1$ then $|z_1| < a$. For $t > t_1$ the control law (19) becomes

$$u_\psi = \arcsin(z_1 + \sigma_b(z_2))$$

Since $z_2 = z_1 + x_{\psi_1}$, it follows that

$$\dot{z}_2 = -\sin(u_\psi) + z_1 = -\sigma_b(z_2)$$

Define the positive function $V_2 = \frac{1}{2} z_2^2$ then $\dot{V}_2$ is

$$\dot{V}_2 = -z_2 \sigma_b(z_2) \tag{21}$$

where $\dot{V}_2 < 0$. For this reason, after a finite time t_2 such that for $t > t_2$ then $|z_2| < b$.

From (21) we notice that $z_2 \to 0$, and recalling (18) we conclude that

$$\begin{aligned} x_{\psi_1} &\to 0 \\ x_{\psi_2} &\to 0 \end{aligned}$$

- **Longitudinal dynamics**: The pitch behavior is governed by the following equation:

$$I_y \ddot{\theta} = -\frac{1}{2} \ell(\cos\xi)(T_1 + T_2 - 2T_3) \tag{22}$$

notice the existence of a nonlinear term which depends on the axial dynamics, i.e. $\cos\xi$. Thus, in order to render this dynamics independent, we should make it robust to this coupling term. For control analysis we assume a normalized value of I_y and $\frac{1}{2}\ell$, now rewriting (22) as

$$\ddot{\theta} = -\delta u_\theta \tag{23}$$

with $\delta = \cos(\xi)$ and $u_\theta = T_1 + T_2 - 2T_3$. δ is considered as a perturbation, which is restricted to $0.54 \leq \delta \leq 1$. This bound arises from the operation range of the servomotor, which was previously bounded to $-1 \leq \xi \leq 1$. The vector-state representation $\dot{X}_\theta = AX_\theta + Bu_\theta$ of (23) is

$$\dot{X}_\theta = \begin{pmatrix} 0 & 1 \\ 0 & 0 \end{pmatrix} \begin{pmatrix} x_{\theta_1} \\ x_{\theta_2} \end{pmatrix} + \begin{pmatrix} 0 \\ -\delta u_\theta \end{pmatrix} \tag{24}$$

where $x_{\theta_1} = \theta$ and $x_{\theta_2} = \dot{\theta}$. Notice that A is not Hurwitz, then, to render it stable, we introduce an artificial input $\bar{u}_\theta$

$$\dot{X}_\theta = \begin{pmatrix} 0 & 1 \\ 0 & 0 \end{pmatrix} \begin{pmatrix} x_{\theta_1} \\ x_{\theta_2} \end{pmatrix} + \begin{pmatrix} 0 \\ -(\bar{u}_\theta - \bar{u}_\theta + \delta u_\theta) \end{pmatrix} \tag{25}$$

with $\bar{u}_\theta = (a_{\theta_1} x_{\theta_1} + a_{\theta_2} x_{\theta_2})$ having $a_{\theta_1}, a_{\theta_2} > 0$, and we obtain

$$\dot{X}_\theta = \begin{pmatrix} 0 & 1 \\ -a_{\theta_1} & -a_{\theta_1} \end{pmatrix} \begin{pmatrix} x_{\theta_1} \\ x_{\theta_2} \end{pmatrix} + \begin{pmatrix} 0 \\ \rho_\theta + \delta u_\theta \end{pmatrix} \tag{26}$$

with $\rho_\theta = a_{\theta_1} x_{\theta_1} + a_{\theta_2} x_{\theta_2}$. Finally we look for an input to deal with δ. We propose $u_\theta = -2\bar{u}_\theta$ to get

$$\dot{X}_\theta = \begin{pmatrix} 0 & 1 \\ -a_{\theta_1} & -a_{\theta_2} \end{pmatrix} \begin{pmatrix} x_{\theta_1} \\ x_{\theta_2} \end{pmatrix} + \begin{pmatrix} 0 \\ \rho_\theta(1-2\delta) \end{pmatrix} \tag{27}$$

choosing this input, we ensure stability for the system for any value within the interval $0.54 \leq \delta \leq 1$

- **Lateral dynamics:** The remaining dynamics is the roll dynamics, which has also the same nonlinear term δ from the axial dynamics. As a result, we follow the same methodology to deduce a controller to stabilize this dynamics.

$$I_x \ddot{\phi} = \frac{1}{2}\sqrt{3}\ell(\cos\xi)(T_1 - T_2) \tag{28}$$

employing similar assumptions as in the previous analysis, we can rewrite (28) as

$$\ddot{\phi} = \delta u_\phi \tag{29}$$

where $u_\phi = T_1 - T_2$. The corresponding vector-state representation $\dot{X}_\phi = AX_\phi + Bu_\phi$, considering the artificial input is written as

$$\dot{X}_\phi = \begin{pmatrix} 0 & 1 \\ 0 & 0 \end{pmatrix} \begin{pmatrix} x_{\phi_1} \\ x_{\phi_2} \end{pmatrix} + \begin{pmatrix} 0 \\ \bar{u}_\phi - \bar{u}_\phi + \delta u_\phi \end{pmatrix} \tag{30}$$

where $x_{\phi_1} = \phi$ and $x_{\phi_2} = \dot{\phi}$. Then, we propose $\bar{u}_\phi = -(a_{\phi_1} x_{\phi_1} + a_{\phi_2} x_{\phi_2})$ and $u_\phi = 2\bar{u}_\phi$ to get

$$\dot{X}_\phi = \begin{pmatrix} 0 & 1 \\ -a_{\phi_1} & -a_{\phi_2} \end{pmatrix} \begin{pmatrix} x_{\theta_1} \\ x_{\theta_2} \end{pmatrix} + \begin{pmatrix} 0 \\ \rho_\phi(1-2\delta) \end{pmatrix} \tag{31}$$

with $\rho_\phi = (a_{\phi_1} x_{\phi_1} + a_{\phi_2} x_{\phi_2})$. This control-input choice stabilizes the system (28) for any value within the interval $0.54 \leq \delta \leq 1$.

IV. Simulation Study

In this section we evaluate the performance of the control laws proposed in the previous sections, numerical simulation is conducted for both control strategies. The parameters employed in the simulation are contained in the table below The initial situation of the vehicle is the following: $(\psi(0),\ \theta(0),\ \phi(0),\ \dot{\psi}(0),\ \dot{\theta}(0),\ \dot{\phi}(0))$=(1,1,-1,1,$\frac{\pi}{4}$,0). The control algorithm utilizes the following control gains:

Parameter	Value
I_x	1 kgm^2
I_y	1 kgm^2
I_z	1 kgm^2
ℓ	0.3 m

TABLE I
Simulation Parameters

Dynamics	Gain 1	Gain 2
Yaw	$a_{\psi_1} = 1$	$a_{\psi_2} = 1$
Pitch	$a_{\theta_1} = 2$	$a_{\theta_2} = 2$
Roll	$a_{\phi_1} = 1$	$a_{\phi_2} = 1$

TABLE II
Control Gains

The performance of the control strategy to achieve an stabilized-attitude flight for the three-rotor mini-UAV is shown on the following set of figures. The figure (3) illustrates the evolution of the heading motion, while figure (4) shows the roll and pitch stabilization and finally, the tilt angle ξ and the perturbation term δ are shown in figure (5). Notice that roll and pitch remain stable despite the perturbation term δ.

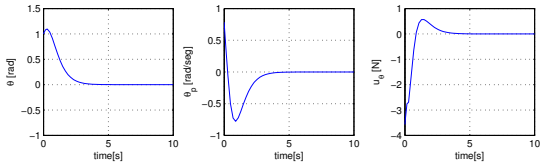

Fig. 3. Performance of heading (yaw)

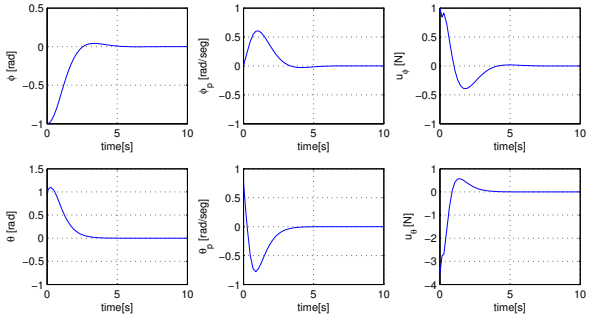

Fig. 4. Performance of horizontal attitude (roll and pitch)

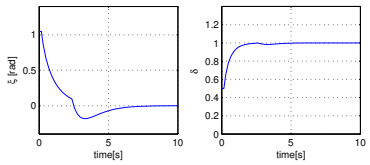

Fig. 5. Performance of tilt angle and perturbation

V. Experimental Setup

A. Aircraft description

The Delta UAV fuselage is made of carbon fiber, measuring approximately $0.3m$ on each side of the Delta. The weight of the vehicle is 0.45 Kg including the battery (Lithium-Polymer). The tilting mechanics is based on electronic servo-motors [see figure 6].

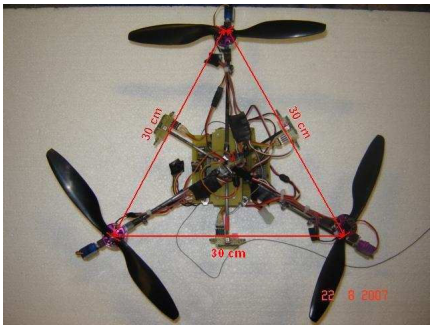

Fig. 6. Dimensions of the Delta UAV.

B. Embedded system

The embedded system includes: an on-board microcontroller, a data acquisition module, and a sensor board. Figure 7 shows the instrumentation of the embedded autopilot.

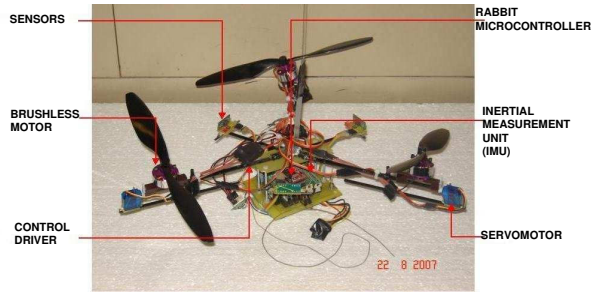

Fig. 7. Principal parts of the Delta UAV.

1) On-board microcontroller (OBM): The flight control law is stored in the microcontroller and the motors are controlled using a PWM signal. The microcontroller processes the feedback signal (IMU), i.e. signal filtering and I-O serial data as well as the pulse width measurement coming from the R/C receptor so that the OBM can include an external user input to perform either manual flight or semi-automatic flight. The selected microcontroller is a 512 Kb flash memory with a 29.4 MHz processor.

2) Data acquisition module (DAQ): The DAQ module links the IMU signal with OMB. It employs a PIC16F873 which features 5 analog input channels with 8 bits resolution and 24 digital I/O channels. This module also incorporate a buffer to interface the PWM signal with the rotor driver.

3) Sensor module (IMU): A customized sensor board was designed and built to provide the PVTOL's angular position (ϕ, θ) and angular rate $(\dot{\phi}, \dot{\theta}, \dot{\psi})$. This board encompasses one dual-axis accelerometer (inclinometers) and three gyroscopes.

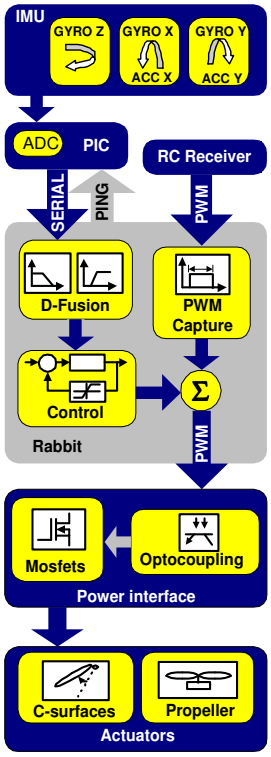

Fig. 8. Block diagram of the embedded autopilot of the Delta UAV.

C. Experimental results

In this section, we show the experimental results corresponding the autonomous attitude-stabilized flight of the Delta UAV. The performance obtained of the Delta UAV are illustrated in the figures 9, 10 and 11.

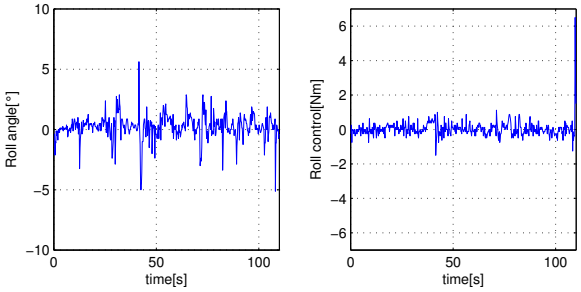

Fig. 9. Roll angle and roll control of the Delta UAV.

VI. Concluding Remarks

We have presented in detail the mathematical model corresponding to the attitude of the proposed configuration. We have built a VTOL rotorcraft based on three tilting rotor that provides a reliable attitude and maneuverability. We have proposed a control strategy robust with respect to dynamic couplings and to the adverse torques $(\Gamma_g^{\mathcal{B}}, \Gamma_d^{\mathcal{B}})$ produced by the gyroscopic-effect and propeller's drag. The resulting control law is simple for embedded purposes.

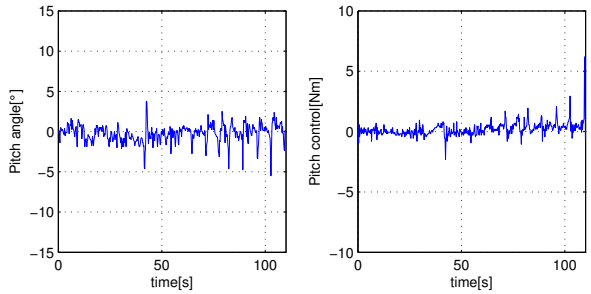

Fig. 10. Pitch angle and pitch control of the Delta UAV.

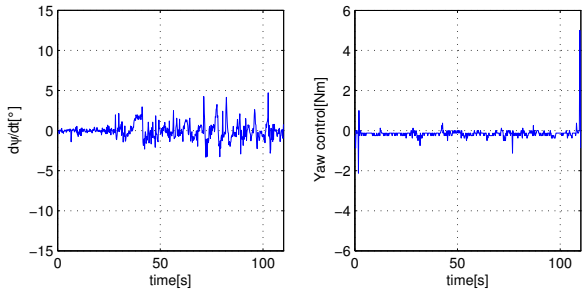

Fig. 11. Yaw angular rate and yaw control.

We have performed a successful autonomous attitude-stabilized flight.

REFERENCES

[1] Fantoni, I. and Lozano, R. (2001). *Non-linear control of underactuated mechanical systems*. Comunications and Control Engineering Series. Springer-verlag. London.

[2] Castillo, P., Dzul, A. and Lozano, R. (2004) *Real-time stabilization and tracking of a four rotor mini rotorcraft*. IEEE Transactions on Control Systems Technology, Vol. 12, Number 4, pp. 510-516.

[3] H. Romero, S. Salazar-Cruz, A. Sanchez, R. Lozano, *A New UAV Configuration Having Eight Rotors: Dynamical Model and Real-Time Control*, 46th IEEE Conference on Decision and Control, December 2007, New Orleans Riverside, New Orleans, Louisiana USA.

[4] G. R. Gress, *Using dual propellers as gyroscopes for tilt-prop hover control*,in Proc. AIAA Biennial Int. Powered Lift Conf. Exhibit, Williamsburg, VA, Nov. 2002, Paper AIAA-2002-5968.

[5] Philippe Rongier, Erwann Lavarec, Franois Pierrot, *Kinematic and Dynamic Modeling and Control of a 3-Rotor Aircraft*, ICRA05, April 18-22, 2005, Barcelona, Spain.

[6] S. Salazar and R. Lozano, *Stabilization and Nonlinear Control for a Novel Trirotor Mini-Aircraft*, ICRA05, April 18-22, 2005, Barcelona, Spain.

[7] H. Goldstein, *Classical Mechanics*, Addison Wesley Series in Physics, Adison-Wesley, U.S.A., second edition, 1980.

[8] Etkin, B. D *Dynamics of flight*. (1959) John Wiley and Sons, Inc. New York.

[9] Teel, A. R. (1996). *A nonlinear small gain theorem for the analysis of control systems with saturations*. IEEE Transactions on Automatic Control 41(9), 1256-1270.

[10] Khalil, H. K. (1995). *Nonlinear Systems*. New York. MacMillan.